Available online at www.sciencedirect.com

ScienceDirect

Current Opinion in
Colloid & Interface Science

Impact of compound drops: a perspective

Nathan Blanken[1,a], Muhammad Saeed Saleem[2,a], Marie-Jean Thoraval[3] and Carlo Antonini[4]

Abstract

Drop interaction with solid surfaces upon impact has been attracting a growing community of researchers who are focusing more and more on 'complex' surfaces and 'complex' drops. Recently, we are observing an emerging research trend related to the investigation of compound drop impact. Compound drops consist of two or more distinct continuous phases sharing common interfaces, surrounded by a third phase. Examples are core–shell and Janus drops. In this review, we address the fundamental aspects of compound drop impact and discuss the current challenges related to experimental testing and numerical simulation of multiphase fluid systems. Furthermore, we provide a perspective on the technological relevance of understanding and controlling compound drop impact, ranging from 3D printing to liquid separation for water cleaning and oil remediation.

Addresses

[1] Physics of Fluids Group, Technical Medical (TechMed) Centre and MESA+ Institute for Nanotechnology, University of Twente, P.O. Box 217, 7500 AE, Enschede, the Netherlands

[2] Physics of Fluids Group, MESA+ Institute for Nanotechnology, University of Twente, P.O. Box 217, 7500 AE, Enschede, the Netherlands

[3] State Key Laboratory for Strength and Vibration of Mechanical Structures, Shaanxi Key Laboratory of Environment and Control for Flight Vehicle, International Center for Applied Mechanics, School of Aerospace, Xi'an Jiaotong University, Xi'an, 710049, China

[4] Department of Materials Science, University of Milano-Bicocca, Via R. Cozzi 55, 20125, Milano, Italy

Corresponding authors: Antonini, Carlo (carlo.antonini@unimib.it); Thoraval, Marie-Jean (mjthoraval@xjtu.edu.cn)

[a] Equal contribution

Current Opinion in Colloid & Interface Science 2021, **51**:101389

This review comes from a themed issue on **Wetting and Spreading**

Edited by **Tatiana Gambaryan-Roisman** and **Victor Starov**

For complete overview about the section, refer Wetting and Spreading

https://doi.org/10.1016/j.cocis.2020.09.002

Keywords

Drop impact, Compound drop, Splashing, Rebound, Wetting, Material 3D printing, Oil–water separation.

Introduction

Drop impact on solid surfaces is an attractive area of study for the complexity of the underpinning physical phenomena, as well as its relevance to a plethora of processes [1,2]. The study of drop collision has traditionally been driven by some classical applications, such as combustion, pesticide delivery, coating fabrication, cleaning, and 2D ink-jet printing on paper. In the past few years, the emergence of some new technologies, such as advanced cell handling [3] and printing for biotechnology [4–6], has further pushed for a better understanding of drop–wall interaction upon impact, as demonstrated by the impressive number of publications reporting either experimental, theoretical or numerical approaches. Performing a simple, but also revealing, 'Scopus' query, we found that more than a thousand papers were related to the term 'drop impact' in 2019 only, with a steady and on-going expansion of the field over the past 15 years (red line in Figure 1a). While most of the literature has focused on the impact of single-phase drops, there is recently a clear emerging trend related to the investigation of compound drops (blue line in Figure 1a).

Compound drop manipulation is of practical interest for any miniaturised microfluidic device [7], with impact on diverse fields, including the food industry and pharmaceutics. Controlling the rheology, in-flight solidification, gelation, and/or curing of drops opens up new possibilities for miniaturised and high-throughput biological assays or the fabrication of new classes of (bio)materials [8]. The subject area distribution for publications related to the keyword 'compound drop' is diverse (see Figure 1b): the majority of the publications is categorised under the areas of physics, engineering and chemical engineering. These are also the traditional subject areas of the wider field of 'drop impact' studies. However, areas such as 'materials science' and 'biochemistry, genetics, and molecular biology' also have a relevant share, confirming the strong interdisciplinarity and broad interest related to the impact of compound drops.

It is important to discuss the expression *compound drops*, because the definition found in the literature is generally wide, with loose boundaries [9,10]. The term is generally used to define drops consisting of two or more distinct continuous phases sharing common interfaces,

Figure 1

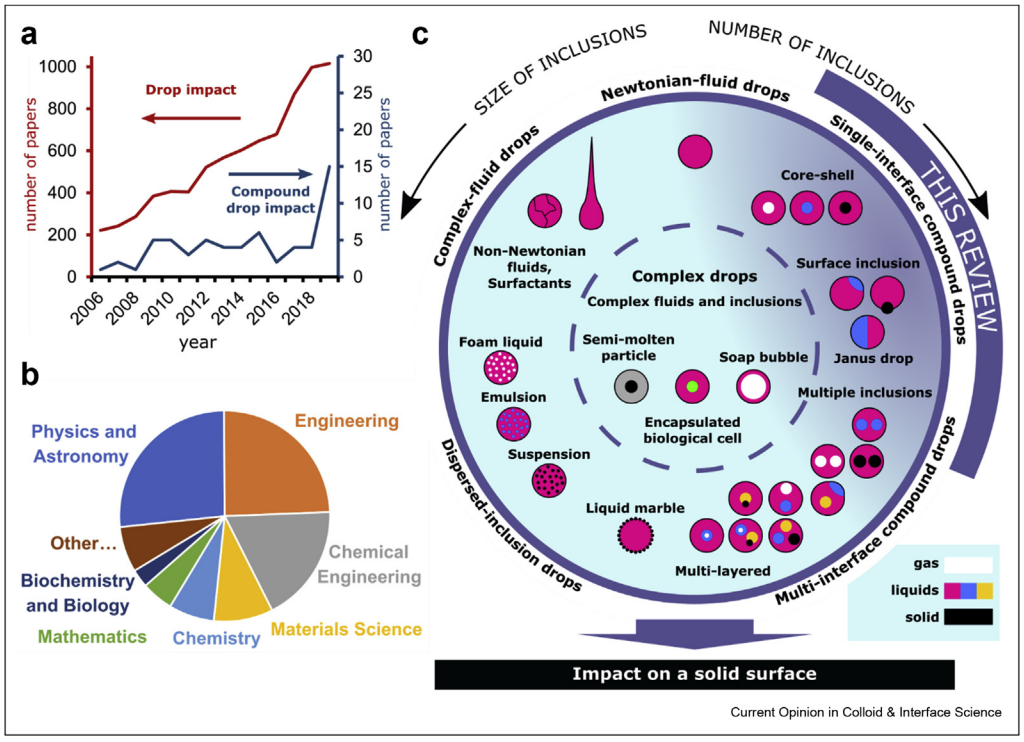

Overview of compound drop research. **(a)** and **(b)**: Statistics related to drop impact publications as extracted from Scopus. **(a)** Number of published documents from 2006 to 2019, using as research query ALL ('drop impact') (red line, left y-scale) and ALL ('drop impact' AND 'compound drop', blue line, right y-scale) (query on scopus.com, April 16th, 2020). **(b)** Documents by subject area. **(c)** Schematic of drop impact research area depending on the drop composition. The core of this review focuses on compound drops where a single interface exists within the drop before impact, e.g. core–shell and Janus drop configurations. The discussion will also be extended to some examples of multi-interface compound drops.

surrounded by a third phase (e.g. air). The dispersed phases can be not only fluid but also solid, in case solid particles are present. Figure 1c presents a schematic overview of the complete field of 'complex' drops, including drops of complex fluids and drops with inclusions. Starting from the top — the simple case of single-phase Newtonian drops — one can move clockwise, increasing the number of inclusions, moving from single-interface and multi-interface compound drops, towards dispersed-inclusion drops (e.g. emulsions) and complex-fluid drops. As the number of inclusions increases, the characteristic size of the inclusions typically decreases.

Compound drops can assume various geometries, depending on the interfacial properties of the phases involved. Some of the simplest geometries are single-interface compound drops, including core–shell and Janus drops, or drops with a single solid-particle inclusion. However, the term compound drop has occasionally been used to describe drops with multiple inclusions, i.e. multi-interface compound drops. The earliest document in which we found the term describes the experimental observations by Darling in 1913 [11] of 'liquid spheres enclosed in a skin of another liquid' and 'mixed vapour and liquid drops', followed by a patent related to capsule preparation for pharmaceutical applications [12]. There is no well-defined boundary between an emulsion, with a high number of dispersed drops, typically in the range 10 nm–100 μm, and a compound drop with a single inclusion or a limited number of dispersed inclusions, for which length scales of the dispersed drops and the compound drop are comparable.

In this article, we discuss the particularities of compound drop impact studies. The article is structured as follows: in Section From single-phase to compound drops, we illustrate how the relevant phenomena observed in single-phase drops, such as spreading, splashing, recoil, jetting and rebound, may be observed in compound drops, highlighting the peculiarities and novel mechanisms associated to the latter. In this section, we will specifically address the drop generation of different types of compound drops, which is a critical issue in experimental studies, and then focus on the physical phenomena resulting from compound drop impacts. In Section From current challenges to future

applications, we provide a perspective on the future. We address major challenges, especially from the numerical point of view, and highlight the application fields of compound drops. Finally, we discuss future directions for research and technology development to improve our physical understanding and to use this knowledge to engineer new materials, processes, and systems.

From single-phase to compound drops

Single-interface compound drop configurations

Many studies on compound drops have focused on two-phase drops. In addition to the two phases of the drop, a third phase is present, namely the medium in which the drop is located (e.g. air). From a heuristic point of view, it makes sense to focus on two-phase systems first, before investigating more complex systems. This approach keeps the number of experimental or numerical parameters as low as possible and allows for a more direct comparison with the vast literature on single-phase drops. The simplest geometries one can think of are core–shell and Janus configurations (see Figure 2). These are single-interface compounds drops, as they both possess a single fluid–fluid interface (not counting the interface with the surrounding medium).

The thermodynamic stability of the core–shell configuration is ruled by the constraint $\sigma_{12} + \sigma_{23} < \sigma_{13}$ [13]. Here, σ_{ij} denotes interfacial tension, and the phases are numbered from inside to outside, as in Figure 2a. In this review, we only consider studies in which the outer medium (phase 3) is air. Water-in-silicone-oil is an example of a configuration that is thermodynamically stable [14]. Thermodynamically unstable configurations can be stabilised by surfactants [15], as in soap bubbles and emulsions. Liquid viscosity can also contribute to stability as it slows down the thinning of the liquid shell [16], as in the case of gas-in-liquid drops, which will be specifically addressed in Section Compound drops with a gas bubble or a single solid particle.

In addition to thermodynamic stability, one has to consider the stability of the relative position of the core phase with respect to the shell phase. We refer to this specifically as mechanical stability. Blanken et al. [14] have shown that only a minor difference in liquid density can have a major effect on the mechanical stability of the compound drop. If the core phase has a higher density than the shell phase, the core tends to accelerate downwards with respect to its surrounding shell when the compound drop falls through air. Similarly, a less dense core tends to move upwards. As will be

Figure 2

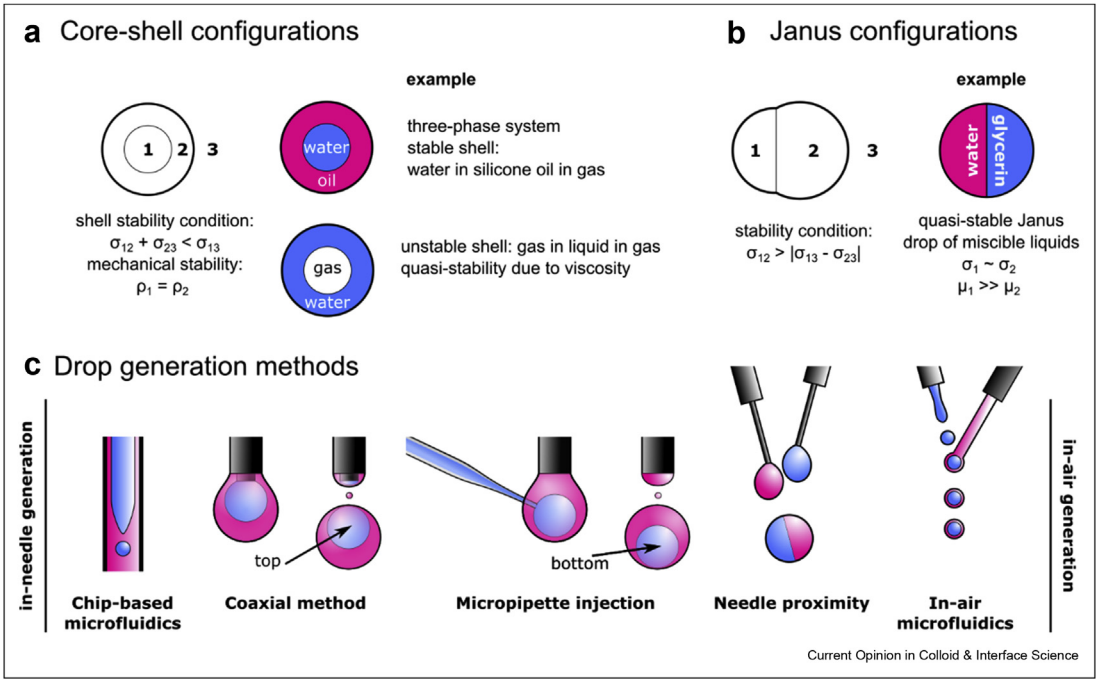

Two-phase compound drop configurations with thermodynamic and mechanical stability conditions, example configurations, and generation methods. (**a**) Core-shell configurations. Water-in-oil drop as described in Ref. [14]. Gas-in-liquid drop as described in Ref. [16]. (**b**) Janus configurations. Glycerin-water drop as described in Ref. [17]. (**c**) Drop generation methods, ordered from left to right, from in-needle methods to in-air methods. Chip-based microfluidics with an inner flow and an outer co-flow [15]. Coaxial generation of drops [14]. Injection of a core drop into a pendant drop by a micropipette [14]. Coalescence of two components due to needle proximity [17]. In-air microfluidics: compound drop generation with two colliding microscale jets [18].

described below, drop geometry can crucially affect drop impact phenomena. Further discussions on the stability of general compound drops can be found in the reviews by Johnson and Sadhal [10] or Gresho [19].

Besides the outer radius and the relative core position, a core–shell compound drop is often characterised by a volume ratio α. Different definitions of α exist in the literature [14,20,21]. Here we use the more common definition $\alpha = \Omega_{core}/\Omega_{tot}$, where Ω_{core} is the volume of the core and Ω_{tot} is the total volume of the compound drop.

If neither of the two liquids wets the other, a triple contact line will exist between the two liquids and the surrounding air, and both drop components will be exposed to the air. Thermodynamically, this configuration is stable if both $\sigma_{12} + \sigma_{23} \geq \sigma_{13}$ and $\sigma_{12} + \sigma_{13} \geq \sigma_{23}$, which can be written more succinctly as $\sigma_{12} \geq |\sigma_{13} - \sigma_{23}|$. This configuration was termed Janus drop (see Figure 2b), in analogy with colloidal Janus particles [22], named after the two-faced Roman god. Although thermodynamically stable liquid Janus drops have been realised in a host liquid [23], the impact of thermodynamically stable fluid Janus drops in air has not been reported in the literature. Nevertheless, Yu et al. [17] have realised a quasi-stable Janus drop in air consisting of miscible liquids. Due to the high viscosity of one of the components, the diffusion length during the drop impact duration remains small compared to the size of the drop, and the drop behaves as a two-component system.

The generation method of a liquid–liquid compound drop is crucial for the post-impact dynamics, as will be detailed below. Different generation methods, schematically presented in Figure 2c, result in varying drop geometries, specifically affecting the vertical position of the core with respect to the shell.

Zhang et al. [15] used a microfluidic device to produce the core drop in the outer liquid before dispensing the compound drop at a simple nozzle. They also used a denser inner liquid, resulting in the settling of the core drop at the bottom of the compound drop during its formation at the nozzle.

Axisymmetric core–shell configurations can also be produced with a coaxial needle [14]. A coaxial needle consists of an inner and an outer needle, through which liquids are independently dispensed from two separate inlets, resulting in the formation of compound drops. When such a system is used, the core is initially located at the top of the shell after pinch-off, see Figure 2c. Drop generation with a coaxial needle allows both for continuous dispensing and for drop-on-demand. Blanken et al. [14] also presented a method that positions the denser core drop at the bottom of the shell. In this method, the tip of a tilted glass micropipette was inserted into a pendant drop, and the core liquid was injected. The pipette was subsequently retracted, shedding off the core, which would settle down on the bottom of the shell due to gravity. By infusing more shell material, pinch-off of the compound drop was induced.

Liu and Tran [21] produced water-in-oil drops with a relatively thin oil shell. They used two needles in close proximity, one dispensing water and the other dispensing oil. The two needles were brought closer together until the two pendant drops touched each other, resulting in the rapid engulfment of the bigger water drop by oil. The resulting compound drop would subsequently pinch off due to its weight. In a similar way, Terwagne et al. [24–26] also used two separate syringes to produce a water-in-oil drop. However, they used an intermediate wire to suspend the drops, let them merge and finally fall under gravity.

Yu et al. [17] used a similar two-needle method to produce Janus drops, see Figure 2c. However, the similar surface tensions of the two liquids and the high viscosity of one of them prevented the formation of a core–shell configuration.

Visser et al. [18] presented an in-air method for producing microscale compound drops. Two separate nozzles produced two streams of liquid that collided in-air. One nozzle was mounted on a piezo-electric driver, resulting in the break-up of one of the jets into a train of monodisperse drops. A compound drop was formed by Marangoni-driven encapsulation of these drops by the intact stream of liquid. They have shown that in-air microfluidics allows for the production of microemulsions, microsuspensions, and 3D (bio)materials, with a throughput that is typically two orders of magnitude higher than chip-based microfluidic methods. A similar system relying on piezo-electric actuation driven rupture of liquid jets to generate compound drops was originally developed by Chiu and Lin [27] with two coaxial liquid jets.

Spreading, splashing, and rebound of core–shell drops

The impact of a core–shell compound drop on a solid surface shows strong similarities with single-phase drop impact, although there are some notable differences. One of the first attempts to systematically explore the behaviour of core–shell drops impacting on a dry, isothermal surface was carried out by Chen et al. [28], who investigated water-in-oil compound drops. They observed splashing and rebound behaviour, phenomena that are known from single-phase studies [1,29]. These observations were later confirmed by others [14,21].

Recently, the spreading and splashing dynamics of an impacting compound drop (water-in-oil) was the subject of two experimental studies by Liu and Tran [21,30]. These dynamical behaviours exist in two separate regimes, characterised by both the Weber number and the volume ratio α. The Weber number of a compound drop was defined as: $We = [\alpha\rho_w + (1-\alpha)\rho_o]D_o V^2/\sigma_o$, where the subscripts w and o denote water and oil, respectively. For $\rho_w = \rho_o$ or $\alpha = 0$ (pure oil), this equation simplifies to the conventional definition of the Weber number. Note that, differently from the original publications, we use the more common definition of α that was given in the previous section. In Ref. [21], the authors show that for thin-shell configurations (approximately $\alpha > 0.8$), the transition to splashing happens at decreasingly lower We for increasing shell thickness (i.e., decreasing α). This transition seems to converge to $We \approx 200$ for $\alpha < 0.8$. Although their article only provides data in the range $0.71 < \alpha < 0.98$, the data in Ref. [14] suggest that the threshold Weber number remains constant down to $\alpha = 0$. Therefore, for thick-shell compound drops ($\alpha < 0.8$), the transition to splashing appears to be similar to the case of a single-phase oil drop, where the core is absent. The splashing dynamics was further characterised in the following study by Liu and Tran [30] in the range $0.91 < \alpha < 0.99$. They proposed a model for the ejection time and velocity of the lamella, based on the model for a single-phase drop [31].

Moreover, Liu and Tran [21] observed, different from single-phase drop impact, the emergence of two lamellas in the spreading regime: the first spreading lamella consisted of oil (shell material), and the second lamella of water (core material). This second lamella gives a second push to the spreading drop and can be observed as a 'shoulder' in the spreading factor, β, as a function of time, see Figure 3a. The time t_b at which this shoulder occurs was found to depend strongly on the volume ratio α.

In the same work, Liu and Tran [21] further studied the maximal spreading factor $\beta_m = D_{max}/D_0$, a characterisation parameter that has been intensively investigated in single-phase drop impact and is relevant for practical applications such as inkjet printing [1,32]. Liu and Tran [21] experimentally showed that the maximum spreading ratio of the compound drops can be expressed as $\beta_m \propto We^{0.28} f(\alpha)$ for $0.71 < \alpha < 0.98$, determining the exponent value by the least-squares fitting method. For a constant value of α, this resembles the scaling law $\beta_m \propto We^k$, observed for single-phase drops in the capillary regime, where values of k in the range $0.25 < k < 0.4$ are typically reported [33]. Such scaling laws were explained recently as a crossover between a capillary regime, where $\beta_m \propto We^{1/2}$, and a viscous regime, where $\beta_m \propto Re^{1/5}$ [1,34–36], with later studies improving this model or identifying its limitations [37–43]. Liu and Tran [21] found that $f(\alpha)$ is minimum for $\alpha \approx 0.85$, which suggests a method for controlling the spreading by varying the volumetric ratio.

The numerical study by Liu et al.[20] explored the maximal spreading of a compound drop impacting on a hydrophobic substrate, varying the interfacial tension between the inner and outer liquids as an additional parameter. They focused on thicker shells, with a range of volume ratios α from 0 to 0.73. They considered both liquids in the drop to have the same density and viscosity, with concentric inner and outer interfaces, and a fixed Reynolds number of 1000. They identified a critical volume ratio, α_c, below which the inner drop does

Figure 3

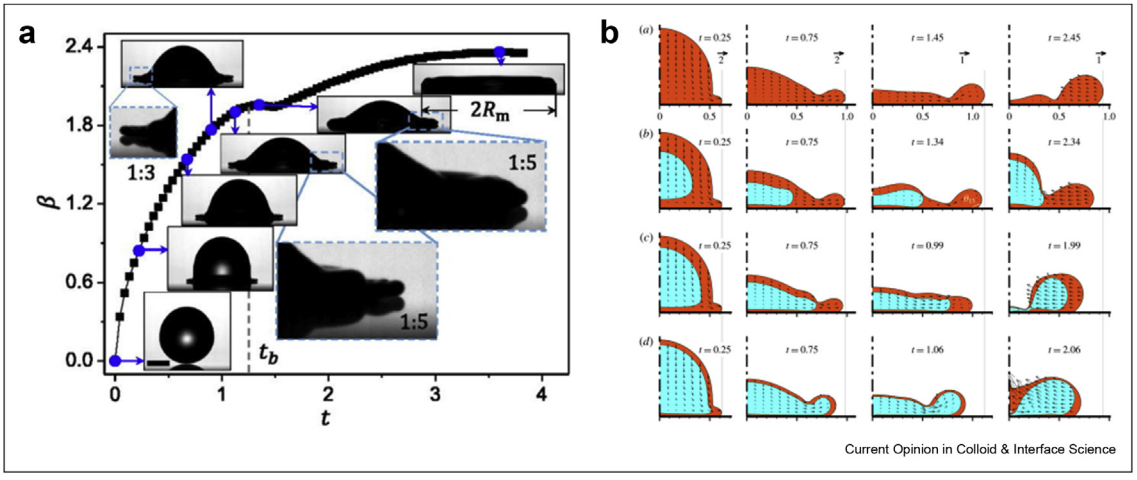

Spreading behaviour of compound drops. (**a**) Spreading dynamics of a water-in-oil compound drop impacting on a solid surface at We = 176, illustrating the formation of two lamellas. Reprinted from Ref. [21], with permission from AIP Publishing. (**b**) Numerical simulations showing the evolution of the spreading dynamics of a compound drop when increasing the volume ratio α. Reprinted from Ref. [20] with permission from Cambridge University Press.

not enter the rim, a phenomenon called 'jammed spreading'. For $\alpha \geqslant \alpha_c$, the inner liquid drop follows the motion of the outer liquid and enters the rim, called 'joint rim formation' (see Figure 3b). They showed that α_c only depends on the interfacial tension between the two drop liquids, and not on the Weber number. Based on these observations, they extended the theoretical model of maximum spreading from pure drops to compound drops [34,35,37], using a modified Weber number We*. In the regime of joint rim formation($\alpha \geqslant \alpha_c$), the modified Weber number We* uses the sum of the interfacial tensions of the two interfaces (core–shell σ_{12} and shell-air σ_{23}, following Figure 2a), instead of only the surface tension of the shell σ_{23}, but does not depend on the volume ratio α. In contrast, in the regime of jammed spreading, the modified Weber number decreases linearly with α between the two limits of a pure drop ($\alpha = 0$, $We^* = We = \rho_1 D_o V^2/\sigma_{23}$) and the regime of joint rim formation ($\alpha \geq \alpha_c$, $We^* = We/(1+\gamma)$, with γ the ratio of surface tensions $\gamma = \sigma_{12}/\sigma_{23}$). Further experiments and simulations will be needed to expand the model to include the effects of different densities and viscosities of the liquids in the drop, as well as the wetting properties or relative position of the core in the shell.

The spreading phase of an impacting drop is generally followed by a recoil phase, which can result in drop rebound. A detailed investigation of the rebound behaviour of core–shell drops was recently performed by Blanken et al.[14], who studied the impact of water encapsulated by a low-viscosity (5 cSt) silicone oil. Most notably, rebound of the water core was observed on both hydrophilic and hydrophobic surfaces (see Figure 4a–c). With single-phase drops, drop rebound is typically only observed on hydrophobic and superhydrophobic surfaces. Blanken et al. [14] attributed the rebound behaviour to the presence of a thin lubricating oil film. Similarities can thus be drawn with impact on lubricated surfaces, such as slippery liquid-infused porous surfaces (SLIPS) or liquid infused surfaces (LIS) [44–46]. In both cases, drop rebound is promoted by a high receding

Figure 4

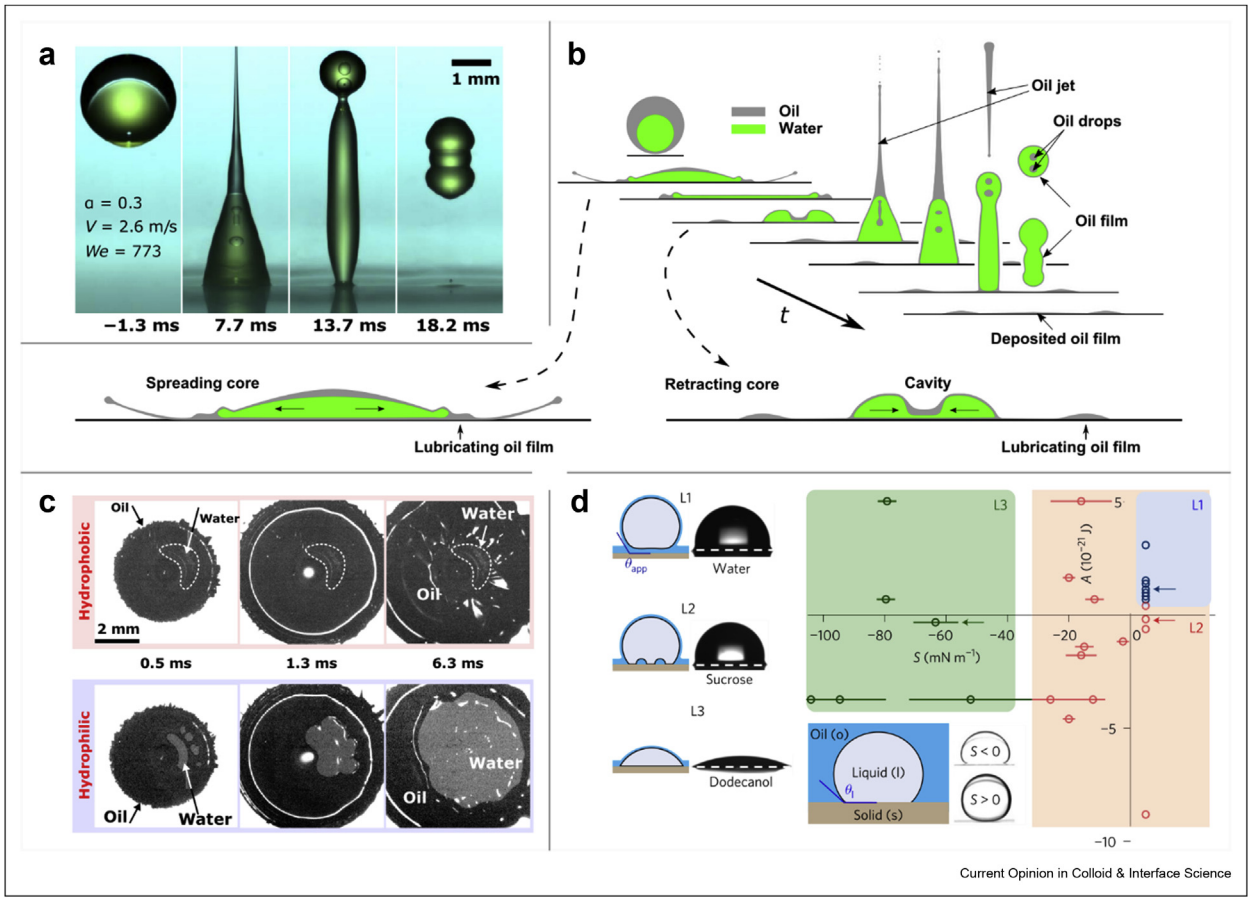

Impact of a water-in-oil drop on a solid surface. (**a**) High-speed colour imaging of an impact event, water dyed green. (**b**) Schematic overview of the series of impact phenomena upon impact, including spreading, splashing, recoil, oil jetting, and core rebound. (**c**) Rupture of the lubricating oil film, bottom view imaging during impact. The contrast is caused by the different reflectivities of the liquids. (**d**) Lubricating-film stability diagram of sessile drops on a lubricated surface. Panels (**a**)–(**c**) adapted from Ref. [14], under the American Association for the Advancement of Science's license to publish, CC BY. Panel (**d**) reprinted from Ref. [48] with permission from Springer Nature.

contact angle, which needs to be higher than 100° for millimetric water drops for rebound to occur [47]. The main difference between water-in-oil compound drop impact and water drop impact on SLIPS/LIS is that a compound drop provides the lubricating layer itself, whereas on SLIPS/LIS the lubricant is already present on the solid surface before impact. Moreover, the rebounding water core remains wetted by the oil throughout the impact event, in accordance with the thermodynamic condition $\sigma_{ow} + \sigma_o < \sigma_w$.

Blanken et al. [14] have shown that core rebound no longer occurs for impacts above a critical impact height. Combined side view and bottom view reflection images (see Figure 4c) provide evidence that this rebound suppression is related to the rupture of the lubricating oil layer. Once the lubricating layer ruptures, the core directly contacts the solid surface. The motion of the resulting contact line over the hydrophilic surface strongly inhibits the recoil of the core, and core rebound is absent. To further highlight the critical role of the lubricating oil layer, impact experiments were also performed on hydrophobic surfaces. On both hydrophilic and hydrophobic surfaces, rupture occurs above a critical impact height. Below this height, no difference in rebound behaviour was observed. However, once the lubricating film ruptures, the rebound strongly depends on the wetting properties of the substrate. As suggested by water drop impact on SLIPS, oil viscosity may play an important role since the impacting drop can more easily displace the oil layer at low viscosity [49].

An important aspect of understanding the rupture of the lubricating oil layer is the thermodynamic stability of the film. Daniel et al.[48] studied the stability conditions for a lubricating film sandwiched between a flat surface and a sessile drop. The stability of the oil film was found to depend both on the spreading constant, $S = \sigma_{ls} - (\sigma_{lo} + \sigma_{os})$, and the Hamaker constant, A, as illustrated in Figure 4d. Here, σ_{ls}, σ_{lo}, and σ_{os} are the liquid/solid, liquid/oil, and oil/solid interfacial tensions respectively. For negative spreading constants, the lubricating film was shown to be unstable, regardless of A. If $-30 < S < 0$, the oil film forms small pockets. If $S < -30$, the oil film is completely expelled. Similar rupture behaviour was observed in the impact experiments by Blanken et al.[14]. For impacts above a critical threshold, on hydrophilic surfaces ($S = -74$ mN/m), water-solid contact starts as small holes in the thin oil film. These holes grow rapidly over time, as visualised in Figure 4c. On hydrophobic surfaces, the oil film may also rupture at high impact velocity. However, the water-solid contact area remains limited.

Although the oil film between the water core and the solid surface is thermodynamically unstable, it stays intact during an impact event, allowing the core to rebound, provided the impact velocity does not exceed a critical value. This temporary stability can be attributed to the lubrication pressure under the core. This pressure is due to the squeezing of the oil film upon impact. The phenomenon is reminiscent of the cushioning air film under a drop on a hot plate (Leidenfrost effect) [50] or under an impacting single-phase drop. De Ruiter et al. [51] have shown that a single-phase drop can bounce on a dry solid surface, independent of the surface wettability, due to the presence of a cushioning air film [52]. Only above a critical impact velocity, the air film is compressed to a critical thickness of approximately 200 nm,resulting in wetting of the solid surface and preventing rebound of the drop. This analogy with single-phase drops could provide more insight into the rebound of compound drops.

In addition to a comparison between impact on hydrophilic and hydrophobic surfaces, Blanken et al.[14] investigated the effect of compound drop geometry on film rupture and rebound behaviour. Drops were generated both with a coaxial needle, which positions the core drop at the top, and through injection with a micropipette, which positions the core drop at the bottom of the compound drop, as was detailed in Section Single-interface compound drop configurations and Figure 2c. It was found that drop production with the coaxial method strongly increases the critical impact height of core-substrate contact, and thus promotes rebound. To understand why, one has to consider the compound drop during the fall. The water core is slightly denser (998 kg/m^3) than the oil drop (913 kg/m^3). Moreover, the compound drop is not in free fall due to air drag. Therefore, the core drop experiences a downward acceleration relative to the shell. Blanken et al.[14] set up a simple force balance to compute the time the core takes to traverse the compound drop from the top to the bottom while the compound drop is falling through air. This time was computed as a function of the water-to-total volume ratio α and translated to the impact height of the compound drop. This theoretical impact height closely matches the experimentally observed core-substrate contact threshold height. This result emphasises that the oil film under the impacting core only ruptures when it is sufficiently thin and stresses the importance of compound drop geometry on drop impact behaviour.

Liquid marbles can be regarded as a more complex example of the core–shell configuration [53]. Liquid marbles are non-sticking drops encapsulated in a shell of colloidal particles which adsorb to the liquid–air interface. As such, they demonstrate elastic properties and the particles may prevent drop coalescence upon impact or externally applied pressure. Two recent studies have addressed the physics of liquid marble impact on solid surfaces [54,55]. Supakar et al. [54] investigated the maximum spreading, identifying a trend $\beta_m \propto We^{1/3}$. This trend is in line with single-phase drop impacts in

the capillary regime, which was discussed above. Additionally, in Ref. [54] it was found that the maximum spreading exhibits no dependence on the particle size or packing structure in the particle shell.

Tenjimbayashi et al. [55] addressed liquid marbles impacting on superhydrophobic surfaces. They showed that surface superhydrophobicity can improve the liquid marble stability. On a hydrophilic surface, recoil and rebound after impact may be hindered if the liquid touches the solid substrate, whereas, on a superhydrophobic surface, rebound still occurs thanks to the Cassie-Baxter wetting. Finally, the impact of composite liquid marbles has been investigated recently by Roy et al. [56], where a water drop was coated by a thin silicone oil layer containing hydrophobic colloidal particles. They demonstrated that such composite liquid marbles show stronger resistance to coalescence compared to classical liquid marbles and exhibit a lower restitution coefficient after impact.

Non-axisymmetric splashing of Janus and multi-interface compound drops

As was discussed above, experiments on the impact of core–shell compound drops suggest that the splashing behaviour of such a drop is similar to the splashing of a single-phase drop consisting of shell liquid. Only for thin-shell compound drops, the splashing seems to be significantly altered. In this section, we focus on the non-axisymmetric impact of millimetric Janus drops. Yu et al. [17] have demonstrated unexpected splashing behaviour for such drops on superamphiphobic surfaces. The one half of such a drop contains a viscous water-glycerin mixture, whereas the other half contains only water. As previously discussed, the two phases remain temporarily distinct despite being miscible since the diffusion length during an impact experiment is considerably smaller than the drop radius. Yu et al. [17] studied the impact configuration in which the interface between the two components is perpendicular to the solid surface (see Figure 5). They found that by attaching a high-viscosity component (glycerin-water) to a low-viscosity component (water), the spreading and splashing of the low-viscosity component was significantly promoted. Conversely, the spreading of the high-viscosity component was inhibited. This behaviour is strikingly different from our intuitive understanding of single-phase drops, for which increasing the viscosity results in reduced splashing due to viscous dissipation [32].

Figure 5

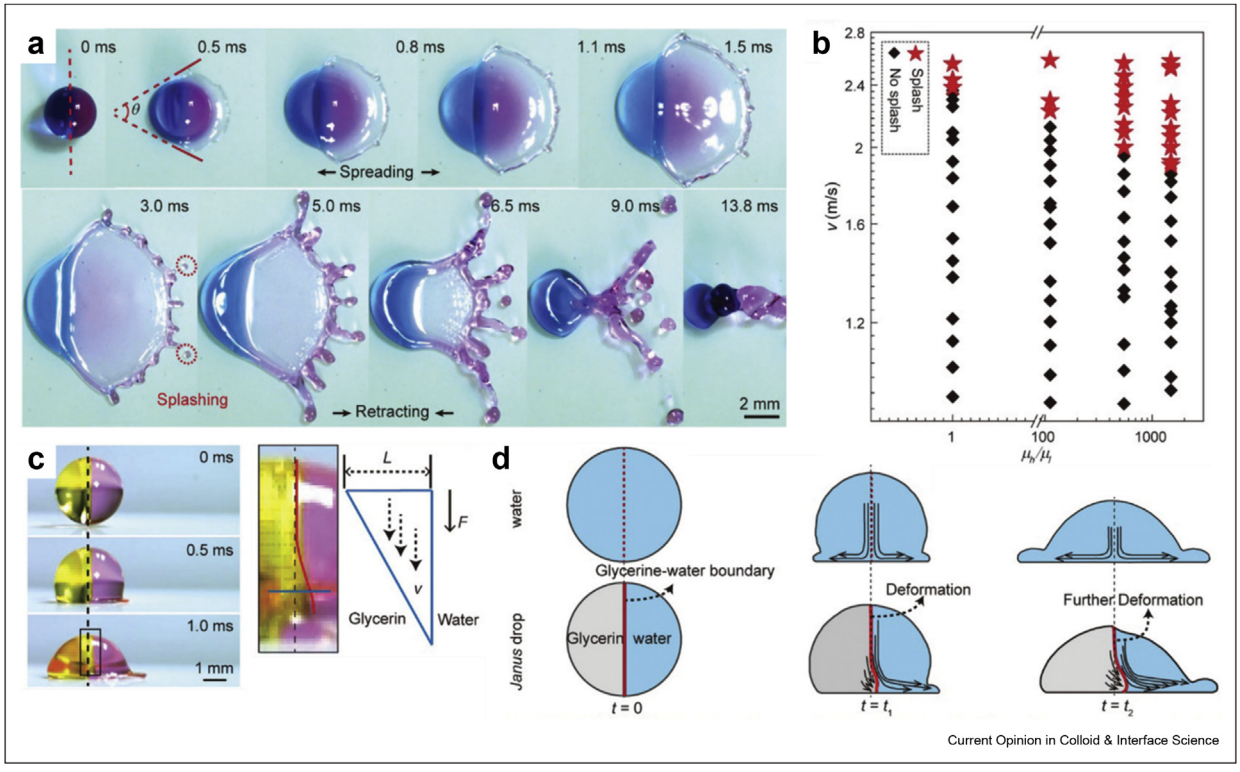

Impact of a Janus drop on a superamphiphobic surface. (**a**) Top view, the glycerin-water mixture is blue, and the water part is red, impact velocity of 2.2 m/s. (**b**) Schematic side view, illustrating the deformation of the interface between the two components. (**c**) Side view of an impacting Janus drop. The inset shows the deformation of the interface and the hypothesised velocity profile along the blue section. (**d**) Schematic of the flow field upon impact. Compilation of figures reprinted from Ref. [17], licensed under a Creative Commons license, CC BY.

Yu et al. [17] quantitively characterised the spreading and splashing behaviour of Janus drop impacts. Firstly, they investigated the splashing threshold of the water component (the minimum impact velocity for which daughter drops detach from the spreading rim): it was found that the splashing threshold decreased for an increasing viscosity of the glycerin mixture. Secondly, by studying the spreading radius of the drop over time, it was found that an increased viscosity of the mixture resulted in a decreased spreading rate of the viscous half. However, the spreading rate of the non-viscous half was increased. Lastly, the Rayleigh-Taylor instability of the rim was characterised by counting the number of corrugations. This instability is observed on the onset of splashing and becomes stronger for higher impact velocities. It was found that the number of corrugations per arc length on the rim of the water component not only increased with increasing impact velocity, as is also the case for single-phase drops, but also with increasing viscosity of the glycerin mixture. In summary, these observations all indicate that increasing the viscosity of the high-viscosity part promotes spreading and splashing of the low-viscosity part.

The authors proposed a theory to account for this behaviour by considering the shear forces on the interface between the two halves of the drop upon impact. Due to viscous dissipation, the flow inside the high-viscosity half is decelerated more abruptly than the flow inside the low-viscosity half, as depicted in Figure 5d. The shear on the interface is $F/A \sim \mu v/L$, where v is the impact velocity, μ is the viscosity of the glycerin mixture, and L is the offset distance over which the vertical flow velocity steeply changes. The higher velocity of the glycerin mixture near the interface guides the flow towards the water half, deforming the interface, displacing the stagnation point of flow towards the glycerin mixture, and boosting the ejection of the water lamella. The authors show that the offset distance L increases linearly with the viscosity μ, resulting in a stronger deformation of the interface, and therefore promoting splashing. In addition to showing this deformation experimentally, they demonstrated it with a volume of fluid method numerical simulation. We note an alternative theory: Gordillo, Sun and Cheng [57] have recently demonstrated that the force produced below an impacting drop scales as $1/\sqrt{\mathrm{Re}}$, which would produce a pressure gradient below the impacting drop from the high-viscosity part to the low-viscosity part. This mechanism could also explain the deformations of the viscous part into the low viscosity part near the solid surface. Further studies quantifying the shear force at the liquid–liquid interface and the pressure distribution on the solid surface are needed to understand these deformations. In conclusion, the work by Yu et al. [17] sheds new light on the phenomenon of splashing, and the authors have presented an intuitive model to explain their observations. Nevertheless, we believe this model requires better verification. The authors envision that their work will be useful for applications where controlled splash is desirable, such as ink-jet printing [58], pesticide deposition [59], and spray cooling process [60].

The axial symmetry is also broken in a multi-interface compound drop: Zhang et al. [15] discovered fine radial jets which are produced when adding denser droplets inside a compound drop. By including multiple denser inner droplets (perfluorohexane) into drops of water-glycerine mixtures, fine radial jets were produced due to a flow-focusing mechanism below the inner droplets during the early phase of impact. A jet can be produced by an inner droplet only if it is located sufficiently far away from the axis of symmetry. Therefore, the axisymmetric configuration, where the compound drop only contains one inner droplet, does not produce such a radial jet. In addition, it was demonstrated that the size of the dimple formed by the inner droplet close to the impact point, plays a critical role in the focusing mechanism: in particular, the dimple diameter controls the width of the jet, and the dimple height controls the focusing effect. The dimple formation was explained with a force balance at the nozzle before releasing the compound drop, between the relative weight of the heavier inner droplet and the capillary pressure of the outer interface. The dimple diameter therefore decreases with the density difference between the inner and outer liquids. This density difference was reduced experimentally by adding salt in the outer phase. It was demonstrated that a lower density difference, and therefore a smaller dimple diameter, could suppress the radial jet formation, confirming the role of the dimple to focus the drop liquid in the jets.

Compound drops with a gas bubble or a single solid particle

In addition to liquid–liquid systems, gas-in-liquid drops are another interesting system, both from a fundamental perspective and for the potential as an additive manufacturing technique of lightweight porous materials and thermal barrier coatings. Recent studies have explored different methods to generate gas-in-liquid compound drops and their impact dynamics [16,61,62]. In this section, we first discuss the physics of gas-in-liquid compound drops, whereas material fabrication and possible applications are discussed in Section Applications.

The earliest work on gas-in-liquid compound-drop impacts was driven by applications in thermal barrier coatings, where hollow particles were demonstrated to improve the deposited coating properties [63]. In another study, the same group demonstrated that a

counter-jet can form during the impact of the compound drop on a solid surface [61] (see Figure 6a).

The presence of surfactants can help stabilise this fundamentally unstable geometry. Soap bubbles represent a particular example of a compound drop, with a thin liquid film surrounding air. Some studies have investigated the coalescence dynamics of soap bubbles [64–67], but their impact dynamics still needs investigation.

Zhu et al. [16] have developed a drop-on-demand system to produce air-in-liquid compound drops without additional surfactant to stabilise the inner bubble. The air bubble was injected into the drop by a short pressure pulse of air through the inner needle of a coaxial needle. The size of the bubble in the resulting compound drop was controlled through the injection pressure of the gas. The authors demonstrated that the deposition of such air-in-liquid compound drops can be hindered by bubble bursting, either before impact, due to air drag resistance, or during impact, due to the rapid deceleration of the compound drop experienced at the surface. They demonstrated that the stability of the bubble in the drop is increased when using a higher viscosity liquid in the shell of the compound drop. Bursting can lead to the emergence of high-velocity vertical jets on top of the drop, either in-flight (see Figure 6b), or during impact. If the air-in-liquid compound drop impacts onto the surface of a pool, the impact can insert the intact bubble into the pool, or split it vertically, leaving two smaller bubbles inside the pool.

Visser et al. [62] have recently presented a new method, referred to as 'direct bubble writing', for the fabrication of polymer foams with configurable bubble size and distribution, density and connectivity (open- or closed-cell structure). Direct bubble writing is based on the rapid generation and patterning of liquid shell–gas core (i.e. gas-in-liquid) drops, produced using a core–shell nozzle (coaxial needle). The liquid was a water-based suspension ink consisting of a polyethylene glycol-

Figure 6

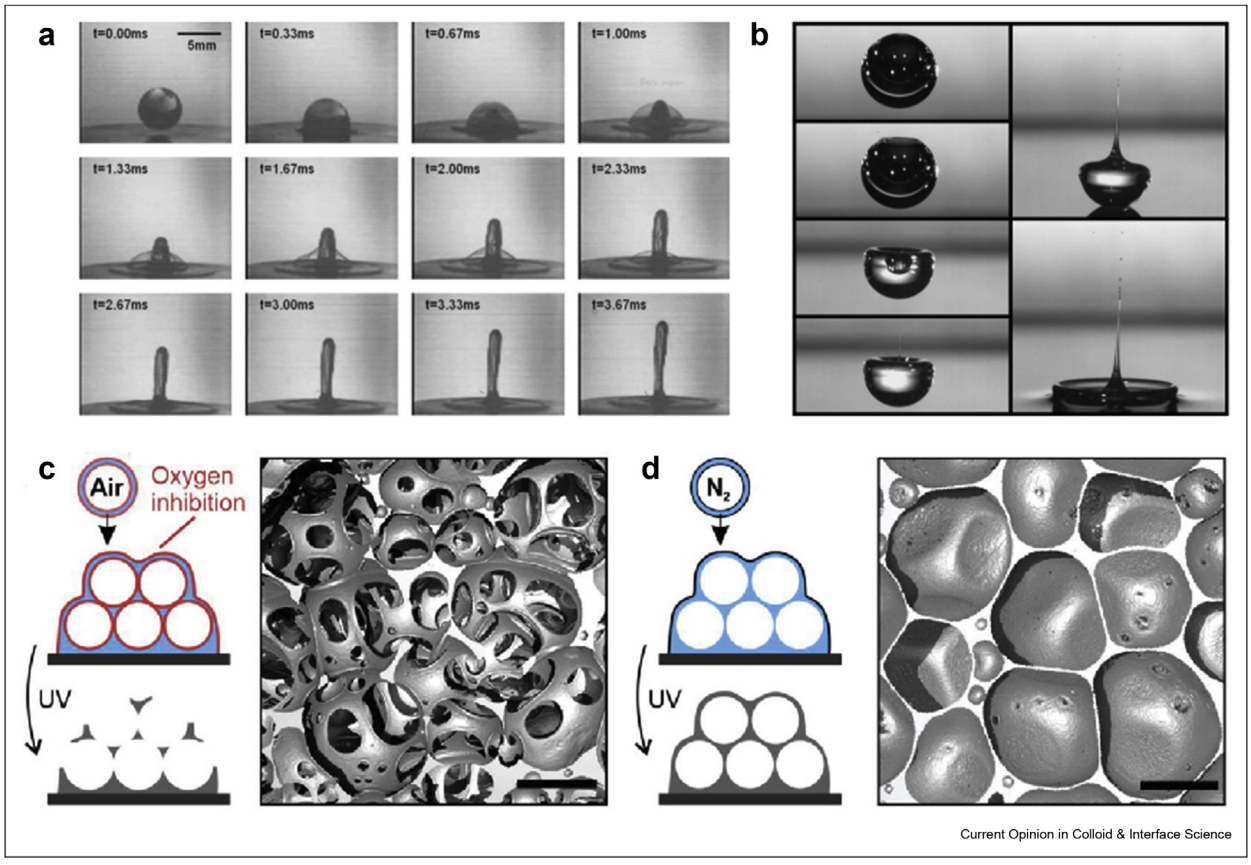

Impact physics and applications of compound drops containing a gas bubble. (**a**) Impact of an air-in-liquid compound drop on a solid surface and the formation of a vertical counter-jet. Reprinted from Ref. [61] with permission from Springer Nature. (**b**) Bursting of an air-in-liquid compound drop before impact, generating a fast vertical jet [16]. Images courtesy of Siqi Zhu. (**c**)–(**d**): Gas-in-liquid drops used for direct bubble writing [62]. (**c**) Open-cell polymer foams formed by printing air-filled bubbles. (**d**) Closed-cell solids formed by printing nitrogen-filled bubbles, resulting in the polymerisation of the intact cell walls. Panel (**c**)–(**d**) reprinted from Ref. [62], with permission from John Wiley and Sons.

diacrylate, a photoinitiator to promote polymerisation after printing, and a surfactant. The ejection behaviour outside the nozzle was primarily determined by two parameters: the liquid flow rate and the gas injection pressure, P_g. In particular, controlled ejection of a bubble train can be achieved by satisfying two conditions. The first condition is on the Weber number: We $>$ 4, to achieve jetting of the liquid. Below this Weber number, dripping is observed. The second condition is on the gas pressure, which has to overcome a total pressure, $P_{tot} = P_l + P_\mu + P_\sigma$. The three partial contributions are the hydrodynamic pressure, P_l, the pressure loss in the nozzle, P_μ, due to viscous effects, and the Laplace pressure, P_σ. The condition $P_g > 0.8\,P_{tot}$ was found to promote train ejection, with the possibility to tune the drop size distribution, from monodisperse bubbles for lower pressures ($2.1 < P_g <$ 2.6 kPa, for the investigated system), to bidisperse bubbles for $2.8 < P_g < 3.4$ kPa. UV light was used to promote polymerisation after impact on the substrate. The final connectivity of the foam could be controlled by changing the gas: the presence of oxygen in air inhibits polymerisation, promoting rupture of the liquid cell wall and eventually leading to an open cell structure (see Figure 6c). Conversely, the use of an oxygen-deficient gas, such as nitrogen, promotes polymerisation and thus the formation of a closed-cell structure (see Figure 6d).

In a following study, Amato et al. [68] improved the 'direct bubble writing' method by replacing the water-based suspension inks by solvent-free and surfactant-free thiol-ene-based inks. While the water-based inks required surfactants to prevent the rupture of the bubbles before reaching the target surface, the higher viscosity thiol-ene-based inks took advantage of the stabilising effect of the liquid viscosity to prevent the bursting of the bubbles, as previously reported by Zhu et al. [16].

Gas-in-liquid compound drops, which contain a low-density inclusion, contrast with compound drops formed by a liquid drop containing a solid particle. If the particle is located at the bottom of the drop, the particle first hits the solid surface. Its rebound can then produce a vertical jet, which is strongly affected by the wetting properties of the particle [69]. If the particle is completely covered by the liquid, the presence of the particle can affect the splashing and spreading of the liquid [70–72].

From current challenges to future applications

Numerical simulations

Numerical simulations have become an important tool for investigating drop impact physics. Simulations allow for precise control of the impact conditions and give full access to the flow dynamics that may be challenging to measure experimentally. However, they are limited by the resolution of the numerical methods and are still not capable of capturing some of the complex three-dimensional multiscale physics involved in drop impact. Most numerical studies on drop impact have focused on the dynamics of single-phase drops. This apparently simple problem already combines two important challenges: the air-liquid interface and the three-phase contact line [73]. Various numerical methods have been developed to capture the dynamics of the interface, including Volume of Fluid, Level Set or Lattice Boltzmann Methods. Interface reconnection events, observed for example in air entrapment or splashing, are especially challenging for sharp interface methods. The interface dynamics create vorticity in a thin layer around the curved interfaces, which is also challenging to capture with numerical methods.

On top of these, numerical studies on compound drops present further challenges with the modelling of the additional phases in the drop, either gas, solid or liquid. When a gas inside an encapsulated bubble differs from the ambient gas, its rupture at the surface of the compound drop requires modelling of mixing and diffusion of gases with different properties. When a second liquid phase is present in the drop, it can form triple lines between fluids. Also, in case the triple lines reach the solid substrate, points where four different phases meet may form. Finally, the presence of a solid phase in the drop requires to model a moving solid together with the interfacial flow and the solid–solid interactions in the case of impact. Although each of these problems has been addressed separately in different numerical methods, only a few studies have combined them to study the dynamics of ternary fluids with moving contact lines [74]. The challenges mentioned above explain why only a very limited number of numerical studies have addressed the problem of compound drop impact [20,75]. The fast development of studies on compound drop impact will likely trigger further developments in the necessary numerical methods.

Applications

Compound drops may soon have an impact on practical applications: here we present some examples of recent applied research in the fields of bulk materials, efficient liquid separation, and drop-based reactors, built on the most recent scientific advances.

Concerning 3D printing, we introduced the 'direct bubble writing' method and the physics behind it in Section Compound drops with a gas bubble or a single solid particle. We saw that the selection of the gas (air, including oxygen, vs. nitrogen) affects the polymerisation, leading to a closed- or open-cell structure.

Figure 7a–d illustrates an example of a large-scale 3D honeycomb structure, printed by the direct bubble writing method. The cell structure can have a significant impact on the bulk material properties, as highlighted in Figure 7e, where the Young's modulus of closed and open-cell structures is presented as a function of the foam relative density $E = f(\rho/\rho_0)$, where ρ_0 denotes bulk density. Let E_0 denote the bulk Young's modulus. According to Ref. [77], for highly porous materials (relative density $\rho_{rel} = \rho/\rho_0 < 0.1$), one expects a power law trend in the form $E = E_0(\rho/\rho_0)^n$. For foams in which bending dominates the deformation behaviour, $n = 2$, while for foams in which deformation occurs by stretching, $n = 1$ [78]. As such, a value $n = 2$ was expected for open-cell solids and $1 < n < 2$ for closed-cell solids with increasingly thin walls [62], with a caveat that foams were produced with a relative density $\rho/\rho_0 > 0.1$. In fact, as can be seen in Figure 7e, higher values for the exponent were found in Ref. [62], i.e. $n \approx 4$ for open-cell and $n \approx 2$ for closed-cells polymer foams. On the one hand, these results confirm that closed-cell structures are less sensitive to density variations, with walls providing good resistance to stress. Indeed, at any given density, the absolute value of the Young's modulus for closed-cell foams is higher than the one for open-cell foams: $E_{closed-cell} > E_{open-cell}$. On the other hand, it shows that for open cells, where the load is borne by struts, a decrease in density significantly deteriorates the Young's modulus. This trend can be advantageous to tune stiffness by several orders of magnitudes over a moderate density range (typically $0.1 < \rho/\rho_0 < 1$).

Figure 7

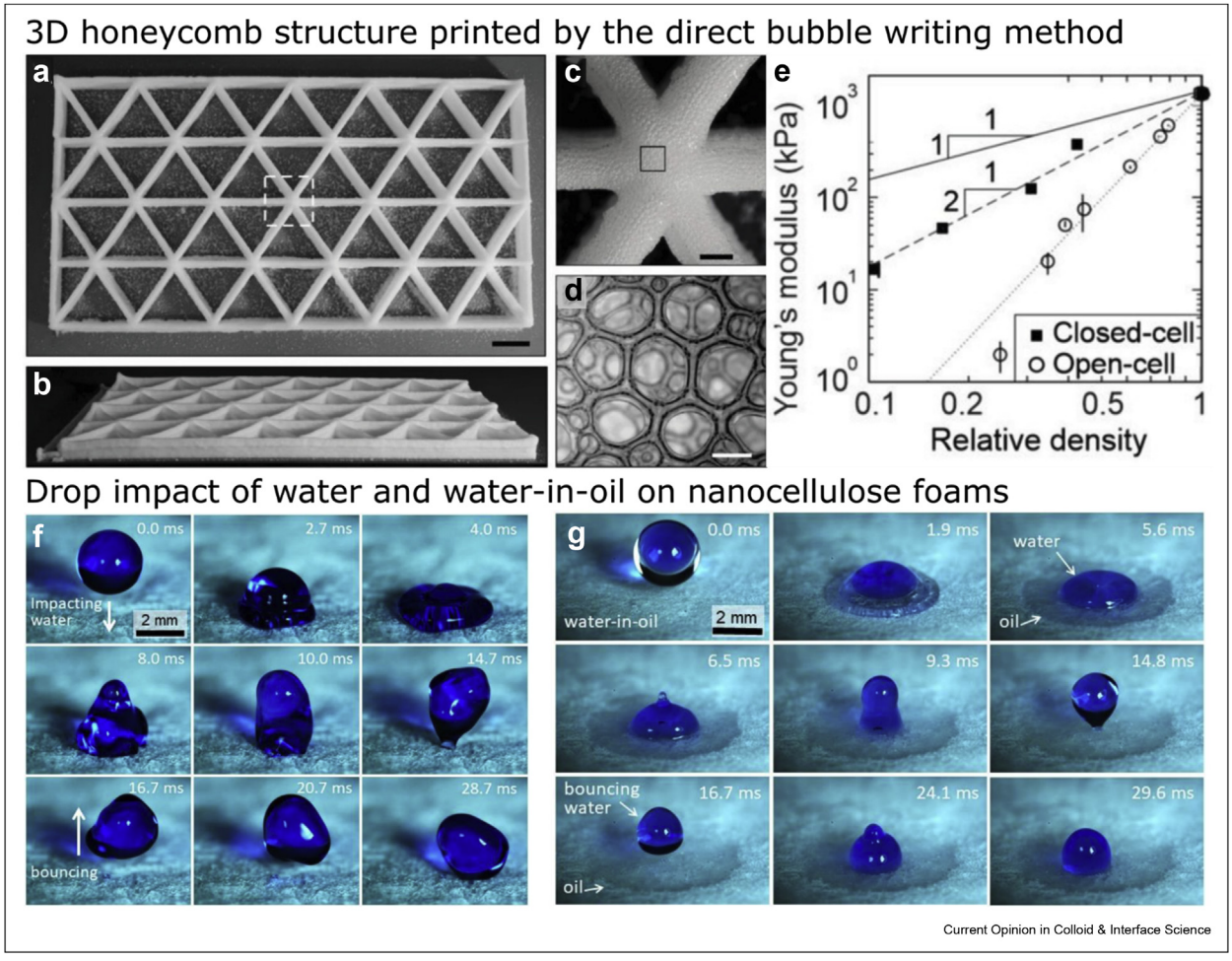

Examples of compound drop applications: (**a**)–(**e**) Large-scale 3D honeycomb structure printed by the direct bubble writing method [62]. (**c**) View of the star-shaped strut connections, with (**d**) detail highlighting the small-scale cell architecture. Scale bars: (**a**) 50 mm, (**c**) 5 mm, (**d**) 0.5 mm. (**e**) Young's modulus as a function of the relative density for open- and closed-cell polymer foams. (**f**)–(**g**) Single-phase and compound drop impact on porous nanocellulose foams [76]. (**f**) High-speed image sequence of a water drop impacting on and rebounding from CNF foams. Impact conditions: drop diameter D = 2.71 mm, impact velocity V = 0.4 m/s. (**g**) High-speed image sequence of a compound water-in-oil (dodecane) drop impacting on CNF foams. Impact conditions: drop diameter D = 2.65 mm, impact velocity V = 1.0 m/s, and water-to-oil ratio $\alpha = 0.3$. Water is blue-stained to improve contrast. Corresponding time for each frame is indicated. Figures (**a**)–(**e**) reprinted from Ref. [62], with permission from John Wiley and Sons. Compilation of figures (f and g) reprinted from Ref. [76], licensed under Creative Commons CC BY.

In addition to the fabrication of porous foams with compound drops, the interaction of compound drops with porous foams is also relevant, particularly in the context of oil remediation. In particular, cellulose nanofibril (CNF) foams have been developed as an absorbing material to separate drops [76] and sprays [79] of water-and-oil mixtures, as demonstrated by compound water-in-oil drop impact experiments [76,79]. On cellulose foams, the combination of surface topography and hydrophobisation induces a superhydrophobic state that can promote rebound both in the case of pure water drops (see image sequence in Figure 7f) and in the case of water-in-oil drops (Figure 7g). As such, the outcome is similar to the case of water-in-oil impact on glass [14] mentioned in Section Spreading, splashing and rebound of core-shell drops. The main difference is that, on a porous material, the oil simultaneously spreads and gets absorbed by the substrate.

Understanding and controlling the complex interplay between spreading and absorption phenomena is challenging and can be done by tuning porosity and the interfacial tensions (water-oil, water-substrate, oil substrate). As an example [76], CNF films with ~70% porosity were exposed to a nebulised mixture of 50:50 vol:vol dodecane and water. The results showed that, after a short time, the film gets impregnated into the film and is retained. Conversely, water drops accumulate on the surface, merge and eventually slide down the surface when the drops reach a critical size and gravity overcomes the capillary adhesion forces. In practice, after the first transient stages, the surface behaves like a SLIPS/LIS liquid impregnated surface [44–46], in which the oil act as a lubricant preventing contact between water and the substrate and promoting drop mobility.

Further promising technologies can be based on liquid marbles. Liquid marbles can be used to build complex shapes and promote liquid self-propulsion [80] and electromagnetically- or mechanically-driven drop motion [81]. Since liquid marbles ensure a controlled and potentially high-throughput handling of small liquid volumes, they have the potential to be used as a platform for a variety of chemical [82] and biomedical [83] applications.

Future directions for research and technology

The studies highlighted above are just the first step towards understanding the impact behaviour of compound drops, and more studies will be needed to have a comprehensive understanding of the impact phenomena. In this section, we want to give an overview of possible future research directions that will challenge researchers for the next few years.

Phase-change phenomena. The interaction of drops with solid surfaces is often associated with phase-change phenomena, such as evaporation, condensation and freezing. As an example, icing, i.e. the solidification of water on a solid surface, is a widely investigated phenomenon. Recently, several research groups have studied the ice nucleation and adhesion on liquid infused surfaces, to understand the role of the infused liquid on controlling, i.e. possibly minimising, ice adhesion to the substrate. The interested reader may refer to the most recent review paper by Roisman and Tropea [84], which is also part of this special issue on 'Wetting and Spreading', or recent references more specific to drop impact [85–89]. Research should continue along the same line with compound drops, e.g. investigating how the presence of a second liquid, such as oil, may influence the water freezing. A similar problem is the solidification of an impacting liquid metal drop [90,91]. The impact of partially molten particles observed in the deposition of thermal barrier coatings is an example where a compound drop geometry is involved together with solidification [70–72].

Leidenfrost boiling. Leidenfrost boiling is a well-known phenomenon related to phase change. It causes surface levitation of drops on a hot substrate, due to evaporation at the liquid–solid interface sustained by the heat transfer from the solid to the liquid. A recent study by Megaridis and coworkers [92] has demonstrated the existence of a novel phenomenon, named explosive boiling, observed for binary drops, which was not observed in single-phase drops. Explosive boiling was observed for intermediate substrate temperatures, between the Leidenfrost temperatures of the more volatile and less volatile component (ethanol and water). The explosion of a Leidenfrost drop was also observed for a surfactant-laden drop [93] or a drop containing microparticles [94]. Such results motivate investigating Leidenfrost impacts for compound drops, following the early studies of [27,95], and exploring the potential for contactless transport of liquids on surfaces [96,97].

Marangoni effect. Another relevant thermocapillary effect phenomenon is the Marangoni effect, which can promote fluid flows at interfaces due to surface tension gradients resulting from temperature gradients. On SLIPS/LIS surfaces [98], temperature gradients can promote the migration of the infused liquid out of surface texture and lead to contact between the liquid to be repelled and the solid substrate. This phenomenon can be relevant for compound drops on surfaces, e.g. during impact of core–shell drops on a hot substrate. Research is needed to understand how Marangoni effects influence the behaviour of the oil layer.

Chemical reactions and cross-linking can be promoted by drop impact. Compound drops can be used to conduct reactions with low volumes or for controlled formation of matter. One example, in the context of natural polymeric structures, was the generation of complex shapes and controlled composition, starting from the collision of aqueous drops of alginate with the surface of a calcium-ion-based liquid [99–101]. This may represent a new route for the fabrication of materials with complex shapes.

Functional coatings and materials. Techniques exploiting compound drops, such as 'in-air microfluidics' [18] or the 'direct bubble writing' method [62,68], have paved the way for the design and fabrication of new functional coatings and materials. We envision further development of compound-drop-based technology, which may enable printing of biopolymers and polysaccharide, for which filament-based 3D printing techniques were recently developed [102,103].

Inclined impacts. Most drop impact investigations focus on normal-incidence drop impact in still air. A comprehensive understanding of the impact dynamics should also include other external forces, such as aerodynamic forces or tangential gravity forces, or tangential velocity components at impact, thus breaking the axisymmetric nature of normal drop impacts. However, only recently attention has moved to testing such conditions, primarily due to the experimental complexity [104–106]. Testing impacts on tilted surfaces is relatively simple but has some limitations: for a given impact speed, increasing the surface tilt angle, α, increases the tangential impact velocity but reduces the normal impact velocity. Also, it is not possible to decouple inertial effects (related to the tangential kinetic energy mV_t^2) from gravitational effects (external force $mg \sin \alpha$, where α is the tilting angle). Alternative and creative solutions have been proposed, such as moving the target on rotating wheels or linearly moving targets [107–109]. However, this system may require: (i) a non-trivial synchronisation of the drop fall with surface motion, (ii) a compromise between spatial resolution and observation window size, to follow the drop evolution after impact with the moving substrates. Nonetheless, such experimental rigs enable exploration of a wider range of impact velocities. They also help to understand the mechanism of drop shedding promoted by external forces, such as gravity and aerodynamic drag, which overcome adhesion (capillary) forces.

Air effects. Air effects have a strong impact on the initial phases of drop impact. It has been shown that splashing can be suppressed by reducing the environmental pressure [1,110–112]. The presence of the air is also responsible for the entrapment of an air disk below the impacting drop [1], as air needs to be drained from underneath the drop before the liquid can touch the substrate. Recent studies have demonstrated that the air compressibility can influence the geometry and dynamics of this air film [113]. These air effects should also be studied for compound drop impacts, especially for the core–shell configuration with the core droplet close to the bottom interface of the drop.

Interfacial surface tensions and the role of surfactants. In the articles discussed above where immiscible fluid-in-fluid systems were investigated, only a few combinations were studied. For example, in Ref. [14] the sum of the interfacial water–oil tension for the investigated system ($\sigma_{ow} = 42$ mN/m) and the oil surface tension, σ_o, is lower than the water surface tension: $\sigma_{ow} + \sigma_o < \sigma_w$. As such, even when the water core rebounds, a thin oil film remains on the surface of the drop. What would happen by changing the interfacial surface tensions? Also, if the interface is stabilised using surfactants that may be present, how would the impact dynamics be affected? Impact could also be performed underwater to evaluate oil emulsion sieving and separation [114].

The boundary between single fluid–fluid interfaces and dispersed emulsions. In this review, we have mostly focused on single-interface compound drops. As schematically presented in Figure 1c, one can move along the circle by increasing the number of particles and decreasing their size, moving from single-interface compound drops, through multi-interface compound drops, towards emulsions. In the context of drop impacts, future research will need to clarify where the transition is between the different configurations, and define what the

Figure 8

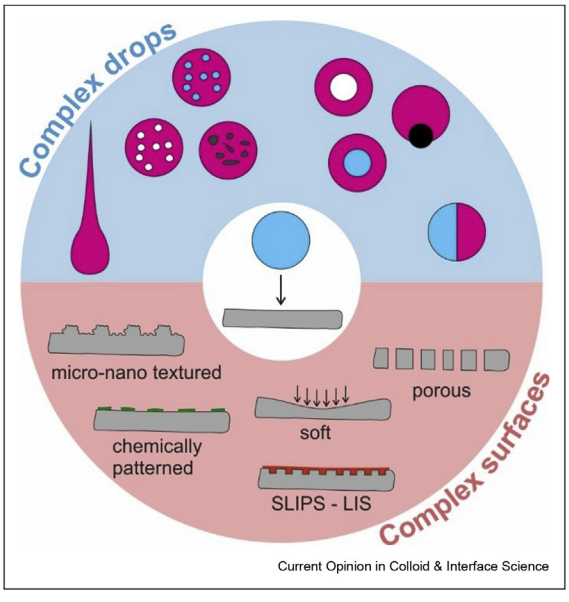

Schematic representation of the drop impact research area, illustrating 'complex' drops impacting on 'complex' surfaces, including: micro-nano textured, chemically patterned, soft, SLIPS/LIS and porous surfaces.

parameters are (drop size, drop density, liquid ratio, etc.) that control the drop impact outcome.

'Complex' drops on 'complex' surfaces. Looking at drop impact on solid surfaces, the simplest scenario one can imagine is the impact of Newtonian fluids, such as water, oil, alcohols, or other organic liquids, on 'simple' smooth surfaces. Degrees of complexity can be introduced by studying the impact behaviour of 'complex' drops on 'complex' surfaces, as schematically visualised in Figure 8. On the one hand, 'complex' drops are a general class that includes compound drops, as well as emulsion drops [115], particle-laden drops [116] and drops consisting of complex liquids [117] (see Figure 1c for a complete overview). On the other hand, of practical interest are the so-called 'complex surfaces' [29], which possess a particular patterning in terms of morphology, chemistry and mechanical properties (e.g. elasticity): recent developments in micro- and nano-technology allow for the fabrication of surfaces with a complex topography (pillars, grooves, nanowires, etc.) and tailored, peculiar wetting characteristics, like superhydrophobicity.

Conclusions

During the past few years, there have been significant efforts to investigate the physics of 'simple' drops and their interaction with 'complex' surfaces. The present understanding of drop collision for such 'simple'" drops forms the basis for better modelling of 'complex' drops, of which compound drops are a subset.

In this review, we have highlighted the emerging trend of research related to the study of compound drops. First, we have highlighted the recent attempts to investigate the fundamental aspects of compound drop impact, mainly focusing on single-interface compound drops, such as core–shell and Janus configurations. Second, we have addressed current challenges which are related to numerical modelling. Multiphase flow simulations present some critical issues, e.g. in the modelling of the three-phase-line dynamics; nonetheless, in the long term, they constitute a unique tool, complementary to experiments, to extend the parameter space of impact conditions and a predictive tool. Third, we have looked into applications in which compound drops play a role, ranging from material fabrication to controlling the behaviour of liquids on surfaces, e.g. for clean-water applications.

For the future, we envision the research will focus on complex drops meeting complex surfaces. More concretely, drops with non-trivial rheological behaviour will be studied on substrates with multitier morphology, heterogeneous wettability, or soft, elastic, or porous characteristics. Also, effects such as thermal effects, phase-change phenomena (solidification, evaporation, condensation, etc.) and chemical reactions will be an important part of the picture. Therefore, addressing future challenges will require a strong interdisciplinary approach and interaction. Advances will rely on the contribution from researchers at the interface between fluid mechanics, chemistry, materials science, physics, and engineering.

The focus of research efforts will be dual-purposed, as usual in science: on the one hand, improve our understanding of drop impacts, one of the most fascinating fluid mechanics phenomena in nature, and on the other hand, control the liquid behaviour to design new materials and processes.

Funding

C.A. and M.-J.T. acknowledge funding from the State Key Laboratory for Strength and Vibration of Mechanical Structures in Xi'an Jiaotong University (SV2019-KF-37). C.A. acknowledges support from the Italian Ministry for University and Research through the Rita Levi Montalcini fellowship for young researchers (2016-NAZ-0233). M.-J.T. acknowledges the financial support from the National Natural Science Foundation of China (grant nos. 11542016, 11702210, and 11850410439) and the Project B18040. M.-J.T. is also supported by the Cyrus Tang Foundation through the Tang Scholar program.

Author contributions

All authors contributed to the structuring and the writing of the manuscript.

Declaration of Competing Interest

The authors declare that they have no known competing financial interests or personal relationships that could have appeared to influence the work reported in this paper.

References

Papers of particular interest, published within the period of review, have been highlighted as:

* of special interest
** of outstanding interest

1. Josserand C, Thoroddsen ST: **Drop impact on a solid surface**. *Annu Rev Fluid Mech* 2016, **48**:365–391, https://doi.org/10.1146/annurev-fluid-122414-034401.

2. Yarin AL, Roisman IV, Tropea C: *Collision phenomena in liquids and solids*. Cambridge, UK: Cambridge University Press; 2017, https://doi.org/10.1017/9781316556580.

3. Foresti D, Nabavi M, Klingauf M, Ferrari A, Poulikakos D: **Acoustophoretic contactless transport and handling of matter in air**. *Proc Natl Acad Sci USA* 2013, **110**:12549–12554, https://doi.org/10.1073/pnas.1301860110.

4. Hendriks J, Visser CW, Henke S, Leijten J, Saris DBF, Sun C, *et al.*: **Optimizing cell viability in droplet-based cell deposition**. *Sci Rep* 2015, **5**:11304, https://doi.org/10.1038/srep11304.

5. Kolesky DB, Truby RL, Gladman AS, Busbee TA, Homan KA, Lewis JA: **3D bioprinting of vascularized, heterogeneous cell-**

laden tissue constructs. *Adv Mater* 2014, **26**:3124–3130, https://doi.org/10.1002/adma.201305506.

6. Foresti D, Kroll KT, Amissah R, Sillani F, Homan KA, Poulikakos D, *et al.*: **Acoustophoretic printing**. *Sci Adv* 2018, **4**: eaat1659, https://doi.org/10.1126/sciadv.aat1659.

7. Guo MT, Rotem A, Heyman JA, Weitz DA: **Droplet microfluidics for high-throughput biological assays**. *Lab Chip* 2012, **12**: 2146–2155, https://doi.org/10.1039/c2lc21147e.

8. Truby RL, Lewis JA: **Printing soft matter in three dimensions**. *Nature* 2016, **540**:371–378, https://doi.org/10.1038/nature21003.

9. Neeson MJ, Tabor RF, Grieser F, Dagastine RR, Chan DYC: **Compound sessile drops**. *Soft Matter* 2012, **8**:11042–11050, https://doi.org/10.1039/c2sm26637g.

10. Johnson RE, Sadhal SS: **Fluid mechanics of compound multiphase drops and bubbles**. *Annu Rev Fluid Mech* 1985, **17**: 289–320, https://doi.org/10.1146/annurev.fluid.17.1.298.

11. Darling CR: **Some further experiments with liquid drops and globules**. *Proc Phys Soc London* 1913, **26**:118–119, https://doi.org/10.1088/1478-7814/26/1/312.

12. Mabbs CE: *Apparatus and process for making capsules*. US321266A. 1940.

13. de Gennes P-G, Brochard-Wyart F, Quéré D: *Capillarity and wetting phenomena: drops, bubbles, pearls, waves*. New York, NY: Springer New York; 2004, https://doi.org/10.1007/978-0-387-21656-0.

14. * Blanken N, Saleem MS, Antonini C, Thoraval M-J: **Rebound of self-lubricating compound drops**. *Sci Adv* 2020, **6**, eaay3499, https://doi.org/10.1126/sciadv.aay3499.
By studying water-in-oil compound drops, the authors demonstrate a self-lubrication mechanism, which leads to the rebound of the core water drop, irrespective of substrate wettability. This is due to lubrication from the oil shell, that prevents contact between the water core and the solid surface. The work is relevant to understand and precisely control compound drop deposition.

15. * Zhang JM, Li EQ, Thoroddsen ST: **Fine radial jetting during the impact of compound drops**. *J Fluid Mech* 2020, **883**:A46, https://doi.org/10.1017/jfm.2019.885.
The authors study the impact of a liquid-in-liquid compound drop onto a solid surface. They discover a new type of radial jetting, produced by a focusing flow mechanism during the impact. The inner droplets deform the drop interface due to gravity. The jet width and velocity depend on the dimple geometry.

16. Zhu S, Kherbeche A, Feng Y, Thoraval M-J: **Impact of an air-in-liquid compound drop onto a liquid surface**. *Phys Fluids* 2020, **32**, 041705, https://doi.org/10.1063/5.0005702.

17. ** Yu F, Lin S, Yang J, Fan Y, Wang D, Chen L, *et al.*: **Prompting splash impact on superamphiphobic surfaces by imposing a viscous part**. *Adv Sci* 2020, **7**:1902687, https://doi.org/10.1002/advs.201902687.
The impact of millimetric Janus drops on superamphiphobic surfaces is studied. The drops consist of a high-viscosity and a low-viscosity component. The authors demonstrate that the presence of the high-viscosity component promotes the splashing of the low-viscosity component. By increasing the viscosity of the high-viscosity part, the threshold impact velocity for splashing is further reduced.

18. Visser CW, Kamperman T, Karbaat LP, Lohse D, Karperien M: **In-air microfluidics enables rapid fabrication of emulsions, suspensions, and 3D modular (bio)materials**. *Sci Adv* 2018, **4**: eaao1175, https://doi.org/10.1126/sciadv.aao1175.

19. Gresho PM: **Some aspects of the hydrodynamics of the microencapsulation route to NIF mandrels**. *Fusion Technol* 1999, **35**:157–188, https://doi.org/10.13182/FST99-A11963919.

20. * Liu H-R, Zhang C-Y, Gao P, Lu X-Y, Ding H: **On the maximal spreading of impacting compound drops**. *J Fluid Mech* 2018, **854**:R6, https://doi.org/10.1017/jfm.2018.702.
The impact of a liquid-in-liquid compound drop is systematically investigated numerically with the ternary-fluid diffuse-interface method. The density and viscosity ratio between the two compound-drop liquids are kept constant, equal to one, while the volume ratio and interfacial tension ratio are varied. The authors extend a previous model for the maximum spreading of a pure drop to this configuration of a compound drop, which compares well with the simulation results.

21. * Liu D, Tran T: **Emergence of two lamellas during impact of compound droplets**. *Appl Phys Lett* 2018, **112**:203702, https://doi.org/10.1063/1.5026821.
The authors documented the emergence of two lamellas in the spreading phase of an impacting water-in-oil compound drop. This two-lamella spreading behaviour exists only for a limited range of Weber numbers and volumetric oil ratios. The first lamella carries oil from the shell, while the second contains water from the core. The second lamella significantly affects the spreading dynamics.

22. Bradley LC, Chen W-H, Stebe KJ, Lee D: **Janus and patchy colloids at fluid interfaces**. *Curr Opin Colloid Interface Sci* 2017, **30**:25–33, https://doi.org/10.1016/j.cocis.2017.05.001.

23. Guzowski J, Korczyk PM, Jakiela S, Garstecki P: **The structure and stability of multiple micro-droplets**. *Soft Matter* 2012, **8**: 7269–7278, https://doi.org/10.1039/c2sm25838b.

24. Terwagne D, Gilet T, Vandewalle N, Dorbolo S: **From a bouncing compound drop to a double emulsion**. *Langmuir* 2010, **26**: 11680–11685, https://doi.org/10.1021/la101096q.

25. Terwagne D, Gilet T, Vandewalle N, Dorbolo S: **Double emulsion in a compound droplet**. *Colloids Surf A: Physicochem Eng Asp* 2010, **365**:178–180, https://doi.org/10.1016/j.colsurfa.2010.02.019.

26. Terwagne D, Mack N, Dorbolo S, Gilet T, Raty J-Y, Vandewalle N: **The mayonnaise droplet**. *Chaos* 2009, **19**, 041105, https://doi.org/10.1063/1.3202626.

27. Chiu S-L, Lin T-H: **Experiment on the dynamics of a compound drop impinging on a hot surface**. *Phys Fluids* 2005, **17**: 122103, https://doi.org/10.1063/1.2139101.

28. Chen RH, Kuo MJ, Chiu SL, Pu JY, Lin TH: **Impact of a compound drop on a dry surface**. *J Mech Sci Technol* 2007, **21**: 1886–1891, https://doi.org/10.1007/BF03177445.

29. Marengo M, Antonini C, Roisman IV, Tropea C: **Drop collisions with simple and complex surfaces**. *Curr Opin Colloid Interface Sci* 2011, **16**:292–302, https://doi.org/10.1016/j.cocis.2011.06.009.

30. Liu D, Tran T: **The ejecting lamella of impacting compound droplets**. *Appl Phys Lett* 2019, **115**, 073702, https://doi.org/10.1063/1.5097370.

31. Riboux G, Gordillo JM: **Experiments of drops impacting a smooth solid surface: a model of the critical impact speed for drop splashing**. *Phys Rev Lett* 2014, **113**, 024507, https://doi.org/10.1103/PhysRevLett.113.024507.

32. Yarin AL: **Drop impact dynamics: splashing, spreading, receding, bouncing…**. *Annu Rev Fluid Mech* 2006, **38**:159–192, https://doi.org/10.1146/annurev.fluid.38.050304.092144.

33. Antonini C, Amirfazli A, Marengo M: **Drop impact and wettability: from hydrophilic to superhydrophobic surfaces**. *Phys Fluids* 2012, **24**:102104, https://doi.org/10.1063/1.4757122.

34. Eggers J, Fontelos MA, Josserand C, Zaleski S: **Drop dynamics after impact on a solid wall: theory and simulations**. *Phys Fluids* 2010, **22**, 062101, https://doi.org/10.1063/1.3432498.

35. Laan N, de Bruin KG, Bartolo D, Josserand C, Bonn D: **Maximum diameter of impacting liquid droplets**. *Phys Rev Appl* 2014, **2**, 044018, https://doi.org/10.1103/PhysRevApplied.2.044018.

36. Gordillo JM, Riboux G, Quintero ES: **A theory on the spreading of impacting droplets**. *J Fluid Mech* 2019, **866**:298–315, https://doi.org/10.1017/jfm.2019.117.

37. Lee JB, Laan N, de Bruin KG, Skantzaris G, Shahidzadeh N, Derome D, *et al.*: **Universal rescaling of drop impact on smooth and rough surfaces**. *J Fluid Mech* 2016, **786**:R4, https://doi.org/10.1017/jfm.2015.620.

38. de Goede TC, de Bruin KG, Shahidzadeh N, Bonn D: **Predicting the maximum spreading of a liquid drop impacting on a solid surface: effect of surface tension and entrapped air layer**. *Phys Rev Fluids* 2019, **4**, 053602, https://doi.org/10.1103/PhysRevFluids.4.053602.

39. Zhao B, Wang X, Zhang K, Chen L, Deng X: **Impact of viscous droplets on superamphiphobic surfaces**. *Langmuir* 2017, **33**: 144–151, https://doi.org/10.1021/acs.langmuir.6b03862.

40. Huang H-M, Chen X-P: **Energetic analysis of drop's maximum spreading on solid surface with low impact speed**. *Phys Fluids* 2018, **30**, 022106, https://doi.org/10.1063/1.5006439.

41. Wildeman S, Visser CW, Sun C, Lohse D: **On the spreading of impacting drops**. *J Fluid Mech* 2016, **805**:636–655, https://doi.org/10.1017/jfm.2016.584.

42. Guo J, Lin S, Zhao B, Deng X, Chen L: **Spreading of impinging droplets on nanostructured superhydrophobic surfaces**. *Appl Phys Lett* 2018, **113**, 071602, https://doi.org/10.1063/1.5034046.

43. Lin S, Zhao B, Zou S, Guo J, Wei Z, Chen L: **Impact of viscous droplets on different wettable surfaces: impact phenomena, the maximum spreading factor, spreading time and post-impact oscillation**. *J Colloid Interface Sci* 2018, **516**:86–97, https://doi.org/10.1016/j.jcis.2017.12.086.

44. Lafuma A, Quéré D: **Slippery pre-suffused surfaces**. *Europhys Lett* 2011, **96**:56001, https://doi.org/10.1209/0295-5075/96/56001.

45. Wong T-S, Kang SH, Tang SKY, Smythe EJ, Hatton BD, Grinthal A, *et al.*: **Bioinspired self-repairing slippery surfaces with pressure-stable omniphobicity**. *Nature* 2011, **477**: 443–447, https://doi.org/10.1038/nature10447.

46. Rykaczewski K, Anand S, Subramanyam SB, Varanasi KK: **Mechanism of frost formation on lubricant-impregnated surfaces**. *Langmuir* 2013, **29**:5230–5238, https://doi.org/10.1021/la400801s.

47. Antonini C, Villa F, Bernagozzi I, Amirfazli A, Marengo M: **Drop rebound after impact: the role of the receding contact angle**. *Langmuir* 2013, **29**:16045–16050, https://doi.org/10.1021/la4012372.

48. Daniel D, Timonen JVI, Li R, Velling SJ, Aizenberg J: **Oleoplaning droplets on lubricated surfaces**. *Nat Phys* 2017, **13**: 1020–1025, https://doi.org/10.1038/nphys4177.

49. Lee C, Kim H, Nam Y: **Drop impact dynamics on oil-infused nanostructured surfaces**. *Langmuir* 2014, **30**:8400–8407, https://doi.org/10.1021/la501341x.

50. Quéré D: **Leidenfrost dynamics**. *Annu Rev Fluid Mech* 2013, **45**: 197–215, https://doi.org/10.1146/annurev-fluid-011212-140709.

51. de Ruiter J, Lagraauw R, van den Ende D, Mugele F: **Wettability-independent bouncing on flat surfaces mediated by thin air films**. *Nat Phys* 2015, **11**:48–53, https://doi.org/10.1038/nphys3145.

52. Kolinski JM, Mahadevan L, Rubinstein SM: **Drops can bounce from perfectly hydrophilic surfaces**. *EPL (Europhys Lett)* 2014, **108**:24001, https://doi.org/10.1209/0295-5075/108/24001.

53. Bormashenko E: **Liquid marbles, elastic nonstick droplets: from minireactors to self-propulsion**. *Langmuir* 2017, **33**: 663–669, https://doi.org/10.1021/acs.langmuir.6b03231.

54. Supakar T, Kumar A, Marston JO: **Impact dynamics of particle-coated droplets**. *Phys Rev E* 2017, **95**, 013106, https://doi.org/10.1103/PhysRevE.95.013106.

55. Tenjimbayashi M, Watanabe Y, Nakamura Y, Naito M: **Exceptional robustness and self-reconfigurability of liquid marbles on superhydrophobic substrate**. *Adv Mater Interfaces* 2020, **7**: 2000160, https://doi.org/10.1002/admi.202000160.

56. Roy PK, Binks BP, Bormashenko E, Legchenkova I, Fujii S, Shoval S: **Manufacture and properties of composite liquid marbles**. *J Colloid Interface Sci* 2020, **575**:35–41, https://doi.org/10.1016/j.jcis.2020.04.066.

57. Gordillo L, Sun T-P, Cheng X: **Dynamics of drop impact on solid surfaces: evolution of impact force and self-similar spreading**. *J Fluid Mech* 2018, **840**:190–214, https://doi.org/10.1017/jfm.2017.901.

58. Wijshoff H: **Drop dynamics in the inkjet printing process**. *Curr Opin Colloid Interface Sci* 2018, **36**:20–27, https://doi.org/10.1016/j.cocis.2017.11.004.

59. Taylor P: **The wetting of leaf surfaces**. *Curr Opin Colloid Interface Sci* 2011, **16**:326–334, https://doi.org/10.1016/j.cocis.2010.12.003.

60. Breitenbach J, Roisman IV, Tropea C: **From drop impact physics to spray cooling models: a critical review**. *Exp Fluid* 2018, **59**:55, https://doi.org/10.1007/s00348-018-2514-3.

61. Gulyaev IP, Solonenko OP: **Hollow droplets impacting onto a solid surface**. *Exp Fluid* 2013, **54**:1432, https://doi.org/10.1007/s00348-012-1432-z.

62. ** Visser CW, Amato DN, Mueller J, Lewis JA: **Architected polymer foams via direct bubble writing**. *Adv Mater* 2019, **31**: 1904668, https://doi.org/10.1002/adma.201904668.
The authors report a new additive manufacturing method, referred to as direct bubble writing, for creating polymer foams with locally programmed bubble size, volume fraction, and connectivity. The method is based on gas-in-liquid drops containing a monomer, which is polymerised during the printing process.

63. Solonenko OP, Gulyaev IP, Smirnov AV: **Thermal plasma processes for production of hollow spherical powders: theory and experiment**. *J Therm Sci Technol* 2011, **6**:219–234, https://doi.org/10.1299/jtst.6.219.

64. Martin DW, Blanchette F: **Simulations of surfactant effects on the dynamics of coalescing drops and bubbles**. *Phys Fluids* 2015, **27**, 012103, https://doi.org/10.1063/1.4905917.

65. Pucci G, Harris DM, Bush JWM: **Partial coalescence of soap bubbles**. *Phys Fluids* 2015, **27**, 061704, https://doi.org/10.1063/1.4923212.

66. Harris DM, Pucci G, Prost V, Casal JQ, Bush JWM: **Merger of a bubble and a soap film**. *Phys Rev Fluids* 2016, **1**, 050505, https://doi.org/10.1103/PhysRevFluids.1.050505.

67. Pfeiffer P, Ohl C-D: **Spreading of soap bubbles on dry and wet surfaces**. *Sci Rep* 2020, **10**:13188, https://doi.org/10.1038/s41598-020-69919-7.

68. Amato DN, Amato DV, Sandoz M, Weigand J, Patton DL, Visser CW: **Programmable porous polymers via direct bubble writing with surfactant-free inks**. *ACS Appl Mater Interfaces* 2020, **12**:42048–42055, https://doi.org/10.1021/acsami.0c07945.

69. Zhao W, Lin S, Chen L, Li EQ, Thoroddsen ST, Thoraval M-J: **Jetting from an impacting drop containing a particle**. *Phys Fluids* 2020, **32**, 011704, https://doi.org/10.1063/1.5139534.

70. Alavi S, Passandideh-Fard M, Mostaghimi J: **Simulation of semi-molten particle impacts including heat transfer and phase change**. *J Therm Spray Technol* 2012, **21**:1278–1293, https://doi.org/10.1007/s11666-012-9804-8.

71. Tabbara H, Gu S: **Numerical study of semi-molten droplet impingement**. *Appl Phys A* 2011, **104**:1011–1019, https://doi.org/10.1007/s00339-011-6510-1.

72. Wu TC-M, Bussmann M, Mostaghimi J: **The impact of a partially molten YSZ particle**. *J Therm Spray Technol* 2009, **18**:957–964, https://doi.org/10.1007/s11666-009-9380-8.

73. Tryggvason G, Scardovelli R, Zaleski S: *Direct numerical simulations of gas-liquid multiphase flows*. Cambridge, UK: Cambridge University Press; 2011, https://doi.org/10.1017/CBO9780511975264.

74. Zhang C-Y, Ding H, Gao P, Wu Y-L: **Diffuse interface simulation of ternary fluids in contact with solid**. *J Comput Phys* 2016, **309**:37–51, https://doi.org/10.1016/j.jcp.2015.12.054.

75. Tasoglu S, Kaynak G, Szeri AJ, Demirci U, Muradoglu M: **Impact of a compound droplet on a flat surface: a model for single cell epitaxy**. *Phys Fluids* 2010, **22**, 082103, https://doi.org/10.1063/1.3475527.

76. Antonini C, Wu T, Zimmermann T, Kherbeche A, Thoraval M-J, Nyström G, *et al.*: **Ultra-porous nanocellulose foams: a facile and scalable fabrication approach**. *Nanomaterials* 2019, **9**: 1142, https://doi.org/10.3390/nano9081142.

77. Gibson LJ, Ashby MF: *Cellular solids: structure and properties*. 2nd ed. Cambridge, UK: Cambridge University Press; 1997, https://doi.org/10.1017/CBO9781139878326.

78. Benedetti M, Klarin J, Johansson F, Fontanari V, Luchin V, Zappini G, *et al.*: **Study of the compression behaviour of Ti6Al4V trabecular structures produced by additive laser manufacturing**. *Materials* 2019, **12**:1471, https://doi.org/10.3390/ma12091471.

79. Orsolini P, Antonini C, Stojanovic A, Malfait WJ, Caseri WR, Zimmermann T: **Superhydrophobicity of nanofibrillated cellulose materials through polysiloxane nanofilaments**. *Cellulose* 2018, **25**:1127–1146, https://doi.org/10.1007/s10570-017-1636-8.

80. Geyer F, Asaumi Y, Vollmer D, Butt H-J, Nakamura Y, Fujii S: **Polyhedral liquid marbles**. *Adv Funct Mater* 2019, **29**, 1808826, https://doi.org/10.1002/adfm.201808826.

81. Fujii S, Yusa SI, Nakamura Y: **Stimuli-responsive liquid marbles: controlling structure, shape, stability, and motion**. *Adv Funct Mater* 2016, **26**:7206–7223, https://doi.org/10.1002/adfm.201603223.

82. Liu Z, Yang T, Huang Y, Liu Y, Chen L, Deng L, *et al.*: **Electro-controlled liquid marbles for rapid miniaturized organic reactions**. *Adv Funct Mater* 2019, **29**, 1901101, https://doi.org/10.1002/adfm.201901101.

83. Oliveira NM, Reis RL, Mano JF: **The potential of liquid marbles for biomedical applications: a critical review**. *Adv Healthc Mater* 2017, **6**, 1700192, https://doi.org/10.1002/adhm.201700192.

84. Roisman IV, Tropea C: **Wetting and icing of surfaces**. *Curr Opin Colloid Interface Sci* 2020 [Accepted].

85. Thiévenaz V, Josserand C, Séon T: **Retraction and freezing of a water film on ice**. *Phys Rev Fluids* 2020, **5**. 041601(R), https://doi.org/10.1103/PhysRevFluids.5.041601.

86. Thiévenaz V, Séon T, Josserand C: **Solidification dynamics of an impacted drop**. *J Fluid Mech* 2019, **874**:756–773, https://doi.org/10.1017/jfm.2019.459.

87. Shang Y, Liu X, Bai B, Zhong X: **Central-pointy to central-concave icing transition of an impact droplet by increasing surface subcooling**. *Int Commun Heat Mass Tran* 2019, **108**:104326, https://doi.org/10.1016/j.icheatmasstransfer.2019.104326.

88. Ghabache E, Josserand C, Séon T: **Frozen impacted drop: from fragmentation to hierarchical crack patterns**. *Phys Rev Lett* 2016, **117**, 074501, https://doi.org/10.1103/PhysRevLett.117.074501.

89. Hu M, Wang F, Tao Q, Chen L, Rubinstein SM, Deng D: **Frozen patterns of impacted droplets: from conical tips to toroidal shapes**. *Phys Rev Fluids* 2020, **5**. 081601(R), https://doi.org/10.1103/PhysRevFluids.5.081601.

90. de Ruiter J, Soto D, Varanasi KK: **Self-peeling of impacting droplets**. *Nat Phys* 2018, **14**:35–39, https://doi.org/10.1038/nphys4252.

91. Gielen MV, de Ruiter R, Koldeweij RBJ, Lohse D, Snoeijer JH, Gelderblom H: **Solidification of liquid metal drops during impact**. *J Fluid Mech* 2020, **883**:A32, https://doi.org/10.1017/jfm.2019.886.

92. Sen U, Roy T, Ganguly R, Angeloni LA, Schroeder WA, Megaridis CM: **Explosive behavior during binary-droplet impact on superheated substrates**. *Int J Heat Mass Tran* 2020, **154**:119658, https://doi.org/10.1016/j.ijheatmasstransfer.2020.119658.

93. Moreau F, Colinet P, Dorbolo S: **Explosive Leidenfrost droplets**. *Phys Rev Fluids* 2019, **4**, 013602, https://doi.org/10.1103/PhysRevFluids.4.013602.

94. Lyu S, Mathai V, Wang Y, Sobac B, Colinet P, Lohse D, *et al.*: **Final fate of a Leidenfrost droplet: explosion or takeoff**. *Sci Adv* 2019, **5**, eaav8081, https://doi.org/10.1126/sciadv.aav8081.

95. Chen R-H, Chiu S-L, Lin T-H: **Resident time of a compound drop impinging on a hot surface**. *Appl Therm Eng* 2007, **27**:2079–2085, https://doi.org/10.1016/j.applthermaleng.2006.11.014.

96. Bouillant A, Mouterde T, Bourrianne P, Lagarde A, Clanet C, Quéré D: **Leidenfrost wheels**. *Nat Phys* 2018, **14**:1188–1192, https://doi.org/10.1038/s41567-018-0275-9.

97. Milionis A, Antonini C, Jung S, Nelson A, Schutzius TM, Poulikakos D: **Contactless transport and mixing of liquids on self-sustained sublimating coatings**. *Langmuir* 2017, **33**:1799–1809, https://doi.org/10.1021/acs.langmuir.6b04377.

98. Bjelobrk N, Girard HL, Bengaluru Subramanyam S, Kwon H-M, Quéré D, Varanasi KK: **Thermocapillary motion on lubricant-impregnated surfaces**. *Phys Rev Fluids* 2016, **1**, 063902, https://doi.org/10.1103/PhysRevFluids.1.063902.

99. Bremond N, Santanach-Carreras E, Chu L-Y, Bibette J: **Formation of liquid-core capsules having a thin hydrogel membrane: liquid pearls**. *Soft Matter* 2010, **6**:2484–2488, https://doi.org/10.1039/b923783f.

100. An D, Warning A, Yancey KG, Chang C-T, Kern VR, Datta AK, *et al.*: **Mass production of shaped particles through vortex ring freezing**. *Nat Commun* 2016, **7**:12401, https://doi.org/10.1038/ncomms12401.

101. Mele E, Fragouli D, Ruffilli R, De Gregorio GL, Cingolani R, Athanassiou A: **Complex architectures formed by alginate drops floating on liquid surfaces**. *Soft Matter* 2013, **9**:6338–6343, https://doi.org/10.1039/c3sm27847f.

102. Siqueira G, Kokkinis D, Libanori R, Hausmann MK, Gladman AS, Neels A, *et al.*: **Cellulose nanocrystal inks for 3D printing of textured cellular architectures**. *Adv Funct Mater* 2017, **27**, 1604619, https://doi.org/10.1002/adfm.201604619.

103. Hausmann MK, Siqueira G, Libanori R, Kokkinis D, Neels A, Zimmermann T, *et al.*: **Complex-shaped cellulose composites made by wet densification of 3D printed scaffolds**. *Adv Funct Mater* 2020, **30**, 1904127, https://doi.org/10.1002/adfm.201904127.

104. Hao J, Lu J, Lee L, Wu Z, Hu G, Floryan JM: **Droplet splashing on an inclined surface**. *Phys Rev Lett* 2019, **122**, 054501, https://doi.org/10.1103/PhysRevLett.122.054501.

105. Hao J, Lu J, Zhang Z, Wu Z, Hu G, Floryan JM: **Asymmetric droplet splashing**. *Phys Rev Fluids* 2020, **5**, 073603, https://doi.org/10.1103/PhysRevFluids.5.073603.

106. García-Geijo P, Riboux G, Gordillo JM: **Inclined impact of drops**. *J Fluid Mech* 2020, **897**:A12, https://doi.org/10.1017/jfm.2020.373.

107. Hao J, Green SI: **Splash threshold of a droplet impacting a moving substrate**. *Phys Fluids* 2017, **29**, 012103, https://doi.org/10.1063/1.4972976.

108. Almohammadi H, Amirfazli A: **Understanding the drop impact on moving hydrophilic and hydrophobic surfaces**. *Soft Matter* 2017, **13**:2040–2053, https://doi.org/10.1039/C6SM02514E.

109. Buksh S, Almohammadi H, Marengo M, Amirfazli A: **Spreading of low-viscous liquids on a stationary and a moving surface**. *Exp Fluid* 2019, **60**:76, https://doi.org/10.1007/s00348-019-2715-4.

110. Xu L, Zhang WW, Nagel SR: **Drop splashing on a dry smooth surface**. *Phys Rev Lett* 2005, **94**:184505, https://doi.org/10.1103/PhysRevLett.94.184505.

111. Jian Z, Josserand C, Popinet S, Ray P, Zaleski S: **Two mechanisms of droplet splashing on a solid substrate**. *J Fluid Mech* 2018, **835**:1065–1086, https://doi.org/10.1017/jfm.2017.768.

112. Burzynski DA, Bansmer SE: **Role of surrounding gas in the outcome of droplet splashing**. *Phys Rev Fluids* 2019, **4**, 073601, https://doi.org/10.1103/PhysRevFluids.4.073601.

113. Li EQ, Thoroddsen ST: **Time-resolved imaging of a compressible air disc under a drop impacting on a solid surface**. *J Fluid Mech* 2015, **780**:636–648, https://doi.org/10.1017/jfm.2015.466.

114. Schutzius TM, Walker C, Maitra T, Schönherr R, Stamatopoulos C, Jung S, *et al.*: **Detergency and its implications for oil emulsion sieving and separation**. *Langmuir* 2017, **33**:4250–4259, https://doi.org/10.1021/acs.langmuir.7b00188.

115. Vernay C, Ramos L, Douzals J-P, Goyal R, Castaing J-C, Ligoure C: **Drop impact experiment as a model experiment to investigate the role of oil-in-water emulsions in controlling the drop size distribution of an agricultural spray**. *At Sprays* 2016, **26**:827–851, https://doi.org/10.1615/AtomizSpr.2015013630.

116. Grishaev V, Iorio CS, Dubois F, Amirfazli A: **Impact of particle-laden drops: particle distribution on the substrate**. *J Colloid Interface Sci* 2017, **490**:108–118, https://doi.org/10.1016/j.jcis.2016.11.038.

117. Oishi CM, Thompson RL, Martins FP: **Impact of capillary drops of complex fluids on a solid surface**. *Phys Fluids* 2019, **31**: 123109, https://doi.org/10.1063/1.5129640.